

Precursor flares in OJ 287

P. Pihajoki¹, M. Valtonen², S. Zola^{3,4}, A. Liakos⁵, M. Drozd⁴, M. Winiarski⁴, W. Ogloza⁴,
D. Koziel-Wierzbowska³, J. Provencal^{6,7}, K. Nilsson², A. Berdyugin¹, E. Lindfors¹, R.
Reinthal¹, A. Sillanpää¹, L. Takalo¹, M.M.M. Santangelo^{8,9}, H. Salo¹⁰, S. Chandra¹¹, S.
Ganesh¹¹, K.S. Baliyan¹¹, S.A. Coggins-Hill¹², and A. Gopakumar¹³

popiha@utu.fi

Received _____; accepted _____

¹Tuorla Observatory, Department of Physics and Astronomy, University of Turku, 21500 Piikkiö, Finland

²Finnish Centre for Astronomy with ESO, University of Turku, 21500 Piikkiö, Finland

³Astronomical Observatory, Jagiellonian University, ul. Orła 171, 30-244 Krakow, Poland

⁴Mt. Suhora Observatory, Pedagogical University, ul. Podchorazych 2, 30-084 Krakow, Poland

⁵Department of Astrophysics, Astronomy and Mechanics, University of Athens, GR 157 84 Zografos, Athens, Hellas, Greece

⁶Department of Physics and Astronomy, University of Delaware, Newark, DE 19716, USA

⁷Delaware Asteroseismic Research Center, Mt. Cuba Observatory, Greenville, DE 19807, USA

⁸O.A.C. Osservatorio Astronomico di Capannori, Via di Valle, 55060 Vorno, Capannori, Italy

⁹I.R.F. Istituto Ricerche Fotometriche, Viale Luporini trav.2 N.111, 55100 Lucca, Italy

¹⁰Department of Physical Sciences, University of Oulu, P.O. Box 3000, 90014 University of Oulu, Finland

¹¹Astronomy & Astrophysics Division, Physical Research Laboratory, Ahmedabad 380009, India

¹²Am Weinberg 16, 63579 Freigericht-Horbach, Germany

¹³Tata Institute of Fundamental Research, Mumbai 400 005, India

ABSTRACT

We have studied three most recent precursor flares in the light curve of the blazar OJ 287 while invoking the presence of a precessing binary black hole in the system to explain the nature of these flares. Precursor flare timings from the historical light curves are compared with theoretical predictions from our model that incorporate effects of an accretion disk and post-Newtonian description for the binary black hole orbit. We find that the precursor flares coincide with the secondary black hole descending towards the accretion disk of the primary black hole from the observed side, with a mean z -component of approximately $z_c = 4000$ AU. We use this model of precursor flares to predict that precursor flare of similar nature should happen around 2020.96 before the next major outburst in 2022.

Subject headings: BL Lacertae objects: individual (OJ 287) – quasars: individual (OJ 287)

1. Introduction

OJ 287 is a blazar at redshift $z = 0.306$ that exhibits nearly periodic double peaked outbursts at intervals of approximately 12 years in the optical regime (Sillanpää et al. 1988, 1996a,b). This periodicity is not exact, as was definitely demonstrated by the observed outbursts in 2005 and 2007 (Valtonen et al. 2006a, 2008a,b). Both the double peaked structure and the dwell in the outburst interval have been successfully explained by a precessing binary black hole model (Lehto & Valtonen 1996; Sundelius et al. 1996, 1997; Valtonen et al. 2011). In this model, the double optical outbursts are caused by a secondary black hole impacting the accretion disk of the primary black hole, twice in one period.

The orbit of the secondary is sufficiently compact and eccentric ($e \sim 0.7$) to bring it close enough to the primary for strong relativistic precession of the orbit (Valtonen & Lehto 1997; Valtonen 2007). The magnitude of the precession has been established at approximately 39.1° per cycle (Valtonen et al. 2010a). The binary black hole with orbital speeds close to 10% of the light speed enabled probing the conservative aspects of general relativistic binary dynamics at the second post-Newtonian order, including the effects of dominant order spin-orbit coupling (Valtonen et al. 2010a). Further, the possibility of testing in the near future general relativity and black hole properties using the binary black hole in OJ 287 makes the detailed understanding of various observational features of the blazar especially important (Valtonen et al. 2011).

In this paper we discuss an aspect of OJ 287 binary black hole which has attracted rather little attention so far. The repeated impacts of the secondary black hole on the accretion disk of the primary create a corona of high velocity gas clouds above the standard geometrically thin but optically thick accretion disk. As the secondary travels through this disk, it may accrete some of the clouds, and these accretion events may lead to quite prominent brightening of the OJ 287 system as whole. They could be contrasted with

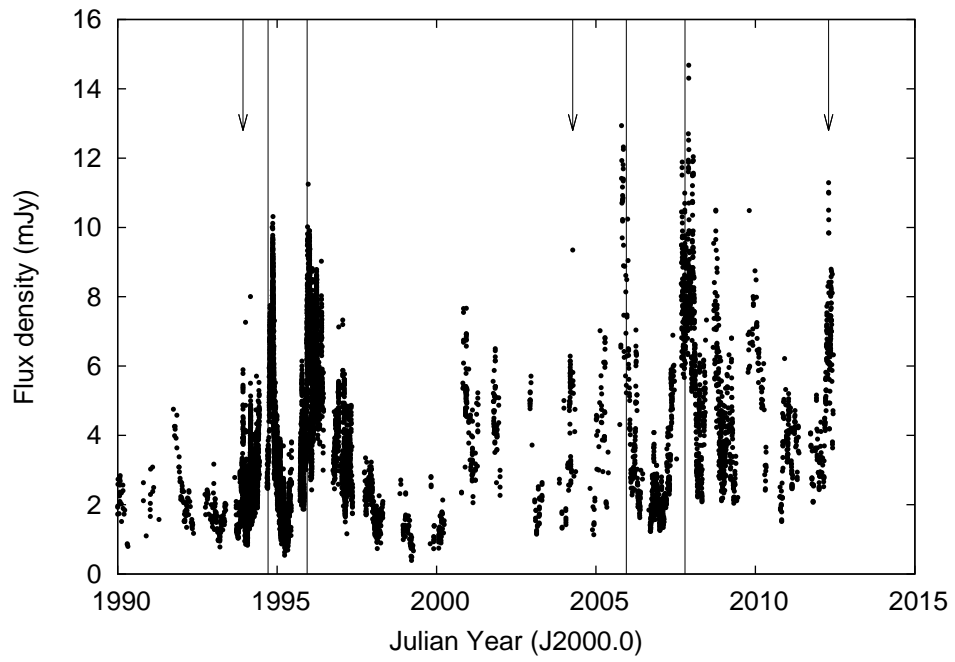


Fig. 1.— Recent light curve of the OJ 287 in V-band equivalent flux. Precursor timings are marked with arrows. Calculated major optical outburst timings of the model in Valtonen et al. (2010b) are marked with vertical lines.

similarly fast brightening events of black holes accreting whole stars, as has been recently reported (Gezari et al. 2012), but with a different timescale and mechanism of action. If such events can be identified, they would allow the detection of the secondary black hole, in addition to the primary which is normally responsible for the emission of OJ 287.

The type of light curve features we will discuss are shown in Figure 1 which displays the optical light curve of OJ 287 since 1990. Besides the double peak structure, indicated by the vertical lines, there are prominent outbursts prior to each cycle called *precursors* by Kidger and Takalo (1993). They are marked by arrows in Figure 1. The first one peaked at 1993.93 and it was studied by Kidger et al. (1994, 1995). The second one peaking at 2004.27 was studied by Valtonen et al. (2006b). They also discussed a possible origin of the precursors. The third precursor occurred only recently, peaking at 2012.29, and the data related to this precursor are reported here. We will also describe two possible scenarios with regard to the origin of precursors and finally settle on a model that seems to fit the limited amount of data.

2. Observations

In addition to the previously published light curve (Valtonen et al. 2009), we have added new datapoints up to the most recent precursor flare. These observations have been made at Tuorla Observatory in Finland (hereafter labelled TUO), Astronomical Observatory of Capannori in Italy (OAC), Astronomical Observatory of the Jagiellonian University (KRK) and the Mt. Suhora Observatory of the Pedagogical University (SUH) in Poland, University of Athens (ATH) in Greece, Mt. Cuba Observatory (MTC) in USA, Mt. Abu Infrared Observatory (MIRO) in India and Liverpool Telescope (LIV) and Kungliga Vetenskapliga Akademien Telescope (KVA) situated at Observatorio del Roque de Los Muchachos in La Palma, Canary Islands, Spain.

The new measurements are catalogued in Table 1. They have been carried out in V, B and R bands, converted to V-magnitudes and then to V-band fluxes (for details, see e.g. Valtonen et al. (2008b)). These light curve points are shown with greater resolution in the lowest panel of Figure 2. The timing of the peak flux is at 2012.29. The two other panels of Figure 2 display the corresponding times around earlier precursors at the same temporal resolution.

We may note that typically there is more than one precursor peak. We will generally discuss the timing of the highest peak, but actual observed maximum height depends on how frequently the observations have been made. The precursors are very rapid phenomena in comparison with the standard double peak outbursts, and therefore the times of maxima may easily pass unobserved. A qualitative definition of a precursor flare can be given as intense flaring activity just before a scheduled major outburst, not exceeding it in brightness. To objectively classify the precursor peaks we note the following: The twin major outbursts typically rise 2.5 mag or more in V-band brightness above the brightness in quiescent state. This quiescent brightness level can be defined as the level under which the V-band brightness doesn't fall, with measurement errors taken into account. This level has been rising gradually; in 1990–1994 it was ~ 1 mJy, in 2000–2005 ~ 1.4 mJy and from 2010 onwards ~ 1.8 mJy. For the precursors, we then have a defining limit of a rise of 2 mag or more in V-band compared to quiescent level. We note that objective classification of precursor flares is not entirely straightforward, as OJ 287 exhibits natural flaring activity induced by the tidal action on the primary accretion by the close passes of the secondary. For the following discussion it is not important which choice of the precursor peak matching the criterion we make.

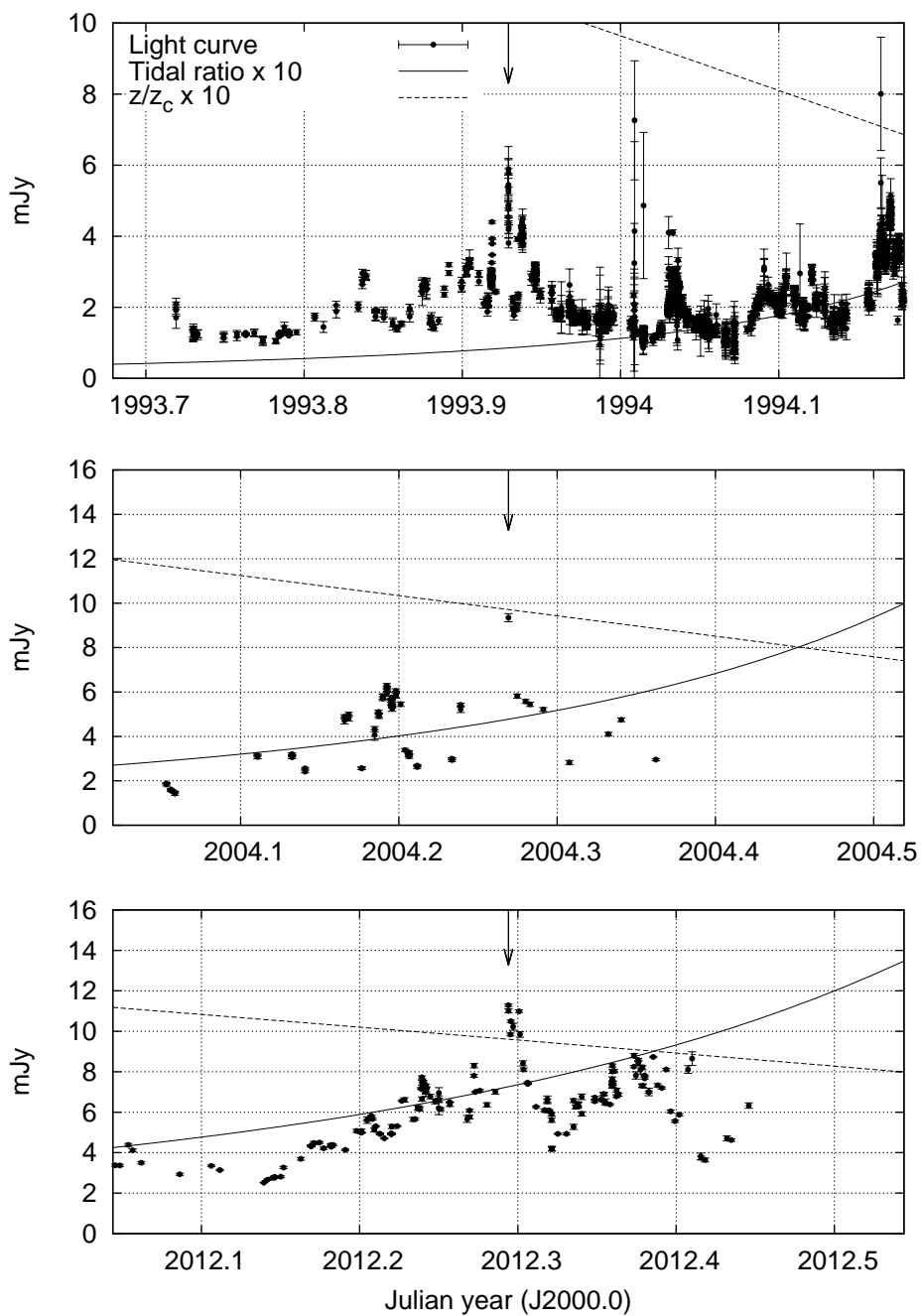


Fig. 2.— Light curve with error bars near the precursor flares. Flare timings are marked with arrows. The solid line gives $10\times$ the tidal ratio while the dashed line shows $10\times$ the height of the secondary above the accretion disk in units of 4084 AU.

2.1. Observations at TUO and KVA

The observations were made with the Tuorla 1.03 m telescope at Tuorla Observatory, Finland and with the 35 cm KVA telescope on La Palma, Canary Islands through the R-band filter. A single observation typically consisted of 3-4 exposures of 60s (Tuorla) or 180s (KVA). The data were reduced in the usual way by first subtracting the bias and dark frames and then dividing by a dome flat-field. The brightness of OJ 287 and star 4 with $R = 13.74$ (Fiorucci et al. 1996) were measured with aperture photometry after which the R-band magnitude of OJ 287 was derived from the measured magnitude difference using color corrections appropriate for the two telescopes.

2.2. Observations at SUH, KRK, ATH and MTC

OJ 287 has been frequently monitored in the R band filter at SUH, KRK and ATH since 2006. Additional data in the R filter has been gathered at MTC in the middle of the 2012 precursor outburst with the 60 cm telescope and an Apogee Alta U47 CCD mounted at the prime focus. The 60 cm telescope equipped also with an Alta U47 CCD installed at the telescope primary focus was used at SUH while the 50 cm telescope and an Andor iKon-L DZ936N-BV camera at KRK. The data at ATH were gathered with the 40 cm Mead telescope and a SBIG ST-10 CCD. Cameras at ATH and KRK are mounted at the Cassegrain foci of the telescopes. We took bias and dark calibration images every night, and whenever possible, sky flatfield images were taken, otherwise, dome flats were used. Each night we took 10–20 frames of OJ 287, usually in the R filter, but on several occasions we measured the blazar in UBVRI wide band filters. *MaximDL* software was used for data gathering at ATH while the *JAstroCam* program (Budyn et al. 2010), developed to run under the Linux OS, was deployed at SUH, KRK and MTC observatories.

The reduction of data taken at the four sites was done by one person to secure uniformity over long period of time. Images of OJ 287 have been corrected for bias, dark and flatfield making use of the *IRAF* package and differential photometry was performed to extract magnitude differences. The *CMunipack* program¹, which is an interface for the *DAOPHOT* package, was applied, stars no. 4 and no. 10 (Fiorucci et al. 1996) served as comparison and check stars, respectively. All individual measurements from each night have been averaged and the standard deviations calculated.

2.3. Observations at OAC

A total of 89 BVRI (17 B, 22 V, 28 R, 22 I) (Johnson/Cousins) CCD frames of OJ 287 were taken at OAC on 18 nights in Spring 2012, from JD 2456015 to JD 2456066, with the 0.30 m $f/10$ telescope equipped with Sbig ST-9XE CCD camera, Sbig CFW-9 filters wheel, Custom Scientific BVRI glass filters, and Sbig AO-8 adaptive optics. On each night also bias frames, master median dark frames, and master median flat field (with both twilight + diffuser, and dome + diffuser) frames were taken.

On some of the nights used for OJ 287, BVRI frames were taken also of the CCD secondary photometric sequence in the so-called dipper asterism region in M67 (Anupama et al. 1994). On two of the nights used for OJ 287, BVRI frames were taken also of the CCD primary photometric sequence around PG1633+099 (Landolt 2009). The frames of M67 and PG 1633+099 sequences were taken in order to derive independent estimates of the coefficients of the colour equations needed to transform OAC's instrumental bvri system to the standard BVRI one; but these frames were not used. Instead, on each observing night, these transformation coefficients were derived from stars of the secondary

¹<http://c-munipack.sourceforge.net>

photometric UBVRI photometric sequence, which is claimed to be in Landolt’s UBVRI system, given by Gonzalez-Perez et al. (2001) for stars just around OJ 287.

BVRI CCD synthetic aperture photometry on the OJ 287 frames was performed at OAC, using the *AIP4 for Win* data reduction software. The stars 9 and 13 of the photometric sequence around OJ 287 established by Gonzalez-Perez et al. (2001) were used respectively as comparison and as check stars. The BVRI (Johnson/Cousins) magnitudes of star 9 and star 13 were taken from table 8 of Gonzalez-Perez et al. (2001). The times of these OAC’s time series were corrected for the heliocentric correction. From the final standard magnitude datapoints, those in B and V bands were used in this publication.

2.4. Observations at MIRO

A total of 1608 exposures were taken in Johnson/Cousins R band on 12 nights in Spring of 2011 and 2012. The CCD used is a liquid nitrogen cooled Pixellent 1296x1152 pixel EEV, Grad 0, with a pixel size of 22 microns and field of view of approx 6.5’x5’. Details of the telescope, observation methods and data reduction pipeline can be found in Baliyan et al. (2005); Chandra et al. (2011).

2.5. Observations at LIV

A total of 298 observations of OJ 287 were taken using CCD frames over a total of 34 nights from JD 2455479.727 to 2456015.357. The observations were taken using the 2 m robotic Liverpool Telescope, equipped with the RATCam optical CCD fitted with clear Sloan r’, Sloan g’ and Bessel B filters. The number of exposures with each filter was: 97 r’, 101 g’, 100 Bessel B. Aperture photometry was then performed on the OJ 287 frames using the *AstroArt 4.0* astronomical image processing software. Finally, the frames were analysed

using an Excel spreadsheet.

For each observation, instrumental and standard magnitudes for OJ 287 were derived from two stars (star 10 and star 4) of the secondary photometric sequence given in Gonzalez-Perez et al. (2001). Star 10 and star 4 were selected as the comparison star and check star respectively.

The published BVRI (Johnson/Cousins) magnitudes of star 10 and star 4 were taken from table 8 of Gonzalez-Perez et al. (2001) and from these the transformed standard magnitudes for the two stars in the Sloan and Bessel filters were derived using transformation formulae in Jester et al (2005) for stars with $R - I < 1.15$.

From the final standard magnitude data points, those in the B band were included in this paper.

3. Possible theoretical explanations

We have calculated the position of the secondary black hole relative to the primary at the times of the precursor flares, using a Post-Newtonian integration scheme of order 3, with binary orbital parameters derived from Valtonen et al. (2010a). Specifically, binary semimajor axis was 11507.957 AU, eccentricity 0.658 and initial precession angle at apocentre 56.3° at epoch 1855.89679 yr. The results shown in Figure 3 indicate that the precursor bursts seem to occur when the secondary is at a constant height of $z_c \sim 4000$ AU above the $z = 0$ plane of the accretion disk of the primary. Thus we have to consider what mechanism would initiate outbursts at this particular orbital phase.

Let us first consider outbursts arising in the primary. They could be initiated by perturbations in the accretion disk; these perturbations propagate to the jet and initiate optical outbursts with about three months time delay (Valtonen et al. 2006b), a reasonable

time interval in a strongly magnetic disk. Such perturbations should start when the tidal perturbation of the secondary on the accretion disk reaches some critical level.

To study this, we have calculated the ratio of the vertical tidal force F_2 , caused by the secondary on an element of the accretion disk immediately below it, to the horizontal tidal force F_1 caused by the primary on the same disk element. The tidal force is proportional to the mass of the black hole and the cube of the distance from it, and the ratio of the forces is thus

$$\frac{F_2}{F_1} = \frac{m_2}{m_1} \frac{r^3}{z^3}, \quad (1)$$

where m_i are the black hole masses, r is the distance from the primary in the plane its accretion disk, and z is the vertical distance of the secondary from the plane of the disk. The tidal ratio (multiplied by 10) has been plotted as a solid line in the three panels of Figure 2. We see that the tidal line describes well the general rise of the activity level in OJ 287, and thus supports the view that this background activity does arise from the primary black hole with its associated disk and jet. However, there is no single threshold level where the precursors start to arise. Thus this explanation does not seem to work for the origin of precursors. It is possible that the tidal process is more complicated than our simple tidal ratio estimate. We will carry out a full tidal perturbation calculation in the next section to check this preliminary conclusion.

The second possibility is that the source of the precursor peak is the secondary black hole. In this scenario the secondary meets a layer of gas clouds at a constant height above the disk, accretes these clouds in individual accretion events, and this produces brightness spikes. To study this scenario, we have plotted the height of the secondary above the accretion disk as a function of time in the three panels of Figure 2 (dashed line). The height is measured in units of $z_c = 4000$ AU (and multiplied by 10 in the display). We see that the constant height is a good predictor for the start of the precursor events, as is also shown by

Figure 3.

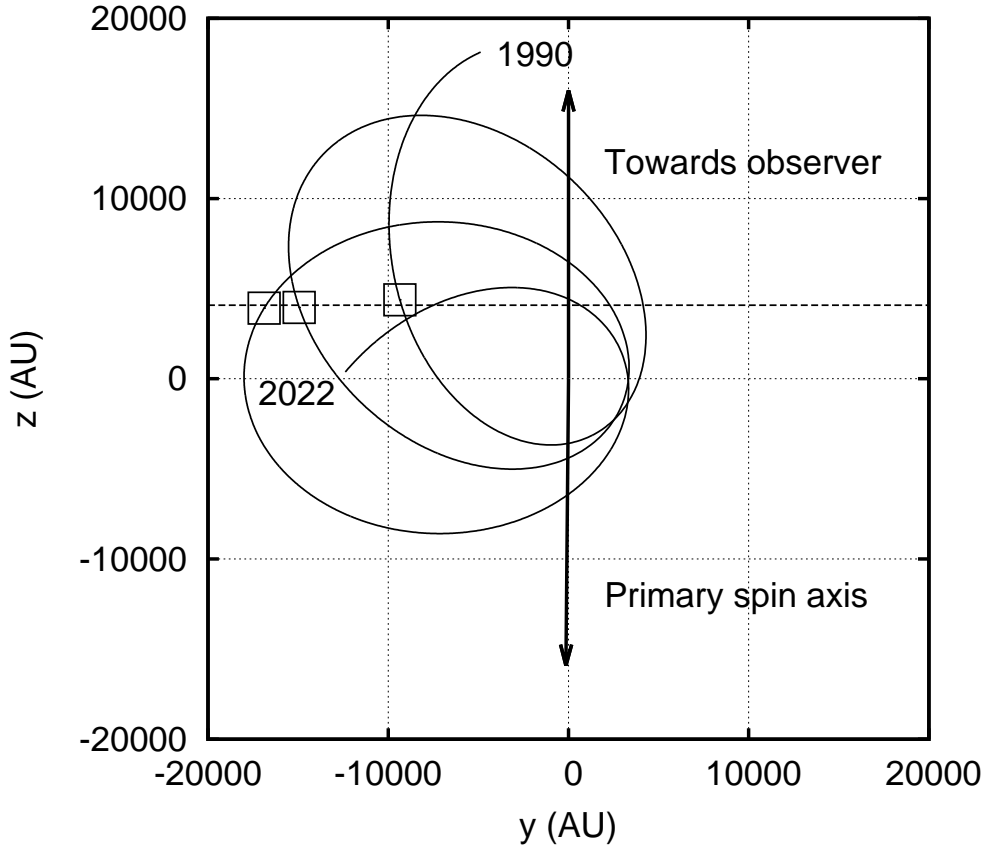


Fig. 3.— Projection of the relative orbit of the secondary black hole to yz -plane. Positions corresponding to precursor flare times are indicated by boxes. The accretion disk of the primary is in the xy -plane.

This result leads us to consider a model where the precursor flares arise in the secondary black hole when it plunges into a gas cloud in the corona of the primary accretion disk. A natural origin for these clouds are the gas clouds pulled off by the secondary from the accretion disk of the primary during previous orbital revolutions. If the secondary impacts these clouds, some of the gas may be accreted by the secondary, with subsequent brightening of its jet.

We may assume the secondary black hole to be maximally spinning, i.e. with Kerr parameter $\chi \sim 1$ and with a mass of $1.4 \times 10^8 M_\odot$ (Valtonen et al. 2010b). This χ value is supported by the observed 228 minute periodicity (Sagar et al. 2004) which is the period of innermost stable orbit for a black hole of this mass and spin. It is also reasonable that the secondary has close to maximum spin as it crosses the primary disk twice in 12 years and every time accretes matter with the same direction of the specific angular momentum, the spin direction of the accretion disk.

The spin of the primary has already been established at $\chi \sim 0.28$ and its mass at $1.84 \times 10^{10} M_\odot$ (Valtonen et al. 2010b). With these values the relative electromagnetic brightness of the secondary versus the primary jet at the times of the outbursts may be rather equal for comparable mass accretion rates (Hawley and Krolik 2006; Neilsen et al. 2011).

Looking at the next time the secondary orbit descends to the height of z_c we can predict the timing of the next precursor flare. The mean value and one sigma limits for z_c give $z_c = (4084 \pm 254)$ AU. From this we find the timing of the next expected precursor burst with one sigma limits to be approximately 2020.96 ± 0.10 . This prediction leaves an ample interval for observation before the next expected major outburst in 2022.

4. Numerical simulation

To simulate the dynamics of the OJ 287 system, we have developed a multiprocessor N-body solver along the lines of Sundelius et al. (1997), but with some significant improvements. The primary improvement is the simultaneous evolution of black hole binary orbits and accretion disk particles around the primary black hole, including interactions between the accretion disk particles themselves.

The accretion disk is modeled as a cloud of point-like particles initialized with a standard vertical $\text{sech}^2(z/z_0)$ distribution, where z_0 is the vertical scale height. The point particles interact gravitationally with both black holes in the binary and with each other through a grid-based viscosity calculation.

For the disk viscosity calculation we use a radially nonuniform polar grid adapted from Miller (1976). In this scheme we define the grid by coordinates u and v such that

$$r(u) = R_c \exp(\alpha u) \tag{2a}$$

$$\theta(v) = \alpha v \tag{2b}$$

where

$$\alpha = \frac{2\pi}{N_\theta} \tag{2c}$$

$$R_c = R_m \exp\left(-\frac{2\pi N_r}{N_\theta}\right). \tag{2d}$$

The parameter R_m defines the maximum radial extent of the grid. Parameters N_r and N_θ then define the number of radial and azimuthal divisions when

$$0 \leq u < N_R \tag{3a}$$

$$0 \leq v < N_\theta. \tag{3b}$$

The benefit of this formulation is that the grid cells are approximately square through the entire radial extent of the grid.

The disk viscosity is calculated in the vertical and radial directions only, using the physical model of Lehto & Valtonen (1996). The kinematic viscosity coefficient ν of the disk gas as a function of the radial distance is obtained from formula

$$\nu = A \left(\frac{r}{\text{pc}}\right)^{3/2} \left(\frac{M}{M_\odot}\right)^{-1/2} \left(\frac{n}{\text{cm}^3}\right)^{-1} \left(\frac{T}{\text{K}}\right)^4, \tag{4}$$

where r is the radial distance, M is the central black hole mass, n is the particle density in the disk, and T is the disk temperature. The last three are functions of r and are obtained from the model in Lehto & Valtonen (1996). For M we use the primary black hole mass from (Valtonen et al. 2010b). Constant $A = 15914 \text{ AU}^2$ in a system of units defined by Solar mass, Julian year and the gravitational constant $G = 1$. The velocity components v_i of each particle in a grid-cell are compared to the mean velocity components \bar{v}_i of all particles in the cell. The viscosity force per unit mass is then calculated from the component differences by the formula

$$f_i = -\alpha\nu(v_i - \bar{v}_i), \quad (5)$$

in which α is the usual parameter in the α -disk theory (Shakura & Sunyaev 1973) and in its subsequent developments (Sakimoto & Coroniti 1981).

Additionally, the solver uses Post-Newtonian approximation scheme to calculate the gravitational interaction of the black hole binary and the forces between the black holes and the accretion disk particles. In these numerical runs, binary dynamics is fully third post-Newtonian order accurate and the required formulas may be found in Valtonen et al. (2010a).

The model was used to calculate particle accretion counts to the primary and secondary black holes. The accretion radii were set to $10r_{\text{sch}}$ for the primary and $100r_{\text{sch}}$ for the secondary, where r_{sch} is the Schwarzschild radius. As found out in Sundelius et al. (1997), changing the accretion radius only affects the scaling of the result, as long as the radius is at or above approximately $10r_{\text{sch}}$. Further, the number of particles escaping beyond $z > 4 \text{stdev}(z)$ vertically was counted, where $\text{stdev}(z) = \pi z_0 / (2\sqrt{3})$, the standard deviation of the $\text{sech}^2(z/z_0)$ vertical distribution. These particles represent such escapes from the disk that end up in the primary or secondary jet as detailed in Valtonen et al. (2006b). The disk vertical scale height used in the simulations was chosen as $z_0 = 260 \text{ AU}$ and the

inner and outer limits of the primary accretion disk were set to 3600 AU and 20600 AU respectively.

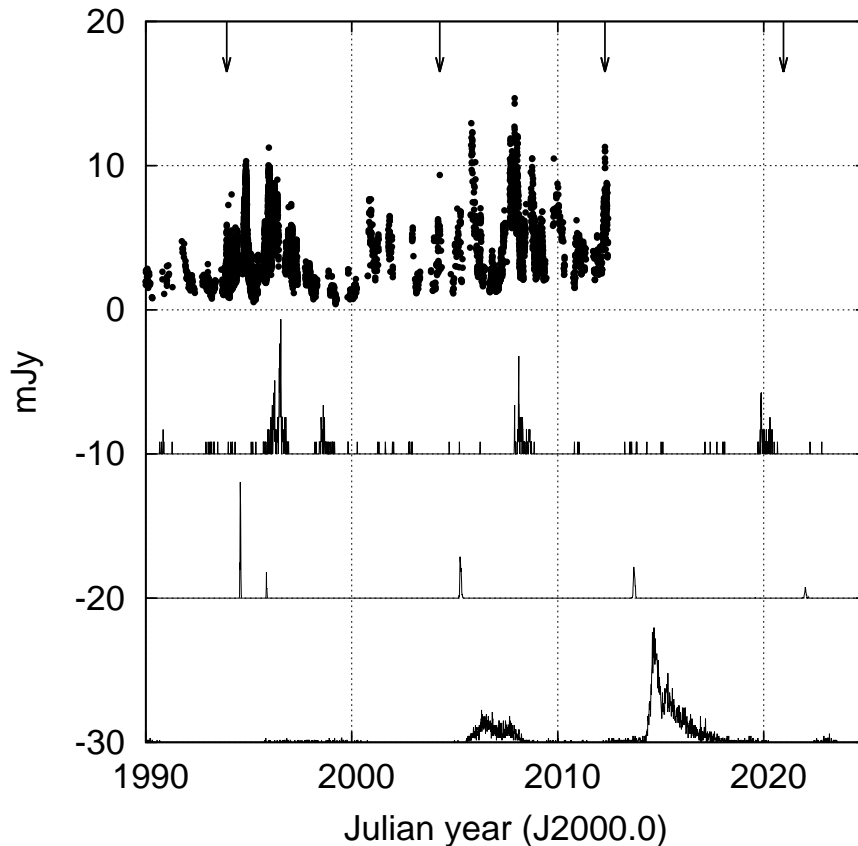


Fig. 4.— Light curve since 1990 (top panel) and accretion counts of primary and secondary black holes, and vertical escape counts (three lower panels, arbitrary scaling, offset by -10 , -20 and -30 , respectively). The three historical and one predicted precursor are indicated by arrows.

The accretion and escape counts since 1990 for the final run with 5×10^5 particles and initial conditions from Valtonen et al. (2010a) can be seen together with light curve data in Figure 4. The major flares and primary and secondary accretion line up well as expected from previous work (Sundelius et al. 1997). The precursor flare timings occur definitely too early in comparison with the particle flows displayed in Figure 4. This applies to the

increases in vertical escapes of the particles from the primary disk (lowest panel in Figure 4) as well as to accretion flows to either of the black holes (the two middle panels in Figure 4).

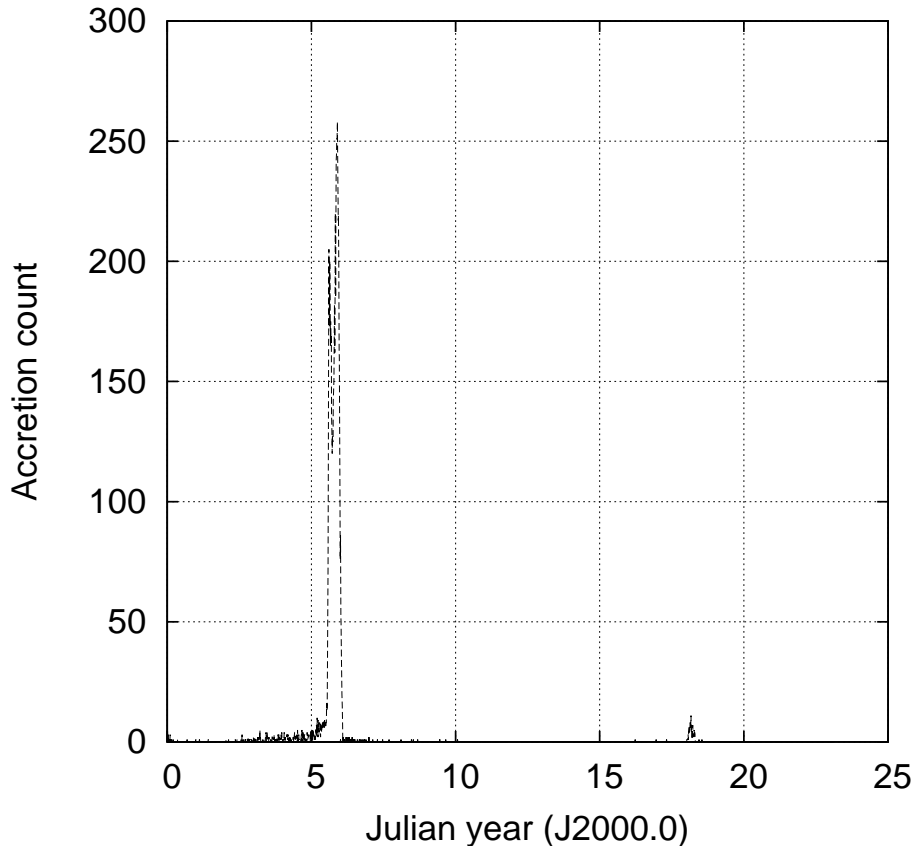


Fig. 5.— Accretion counts of the primary (solid line) and the secondary (dashed line) in a simulation of a circumsecondary disk with a radius of 150 AU.

To study the tidal effect of the primary on the secondary and the proposed coronal gas cloud impacts in more detail, we used the code to simulate the interaction between the secondary and a circumsecondary disk and a cloud of particles representing a coronal cloud. Two representative simulations were chosen, with both using initial conditions from Valtonen et al. (2010a) for the binary. For these simulations, the secondary accretion radius was set to $10r_{\text{sec}}$, where r_{sec} is the Schwarzschild radius. The interparticle gridded viscosity calculation was not used.

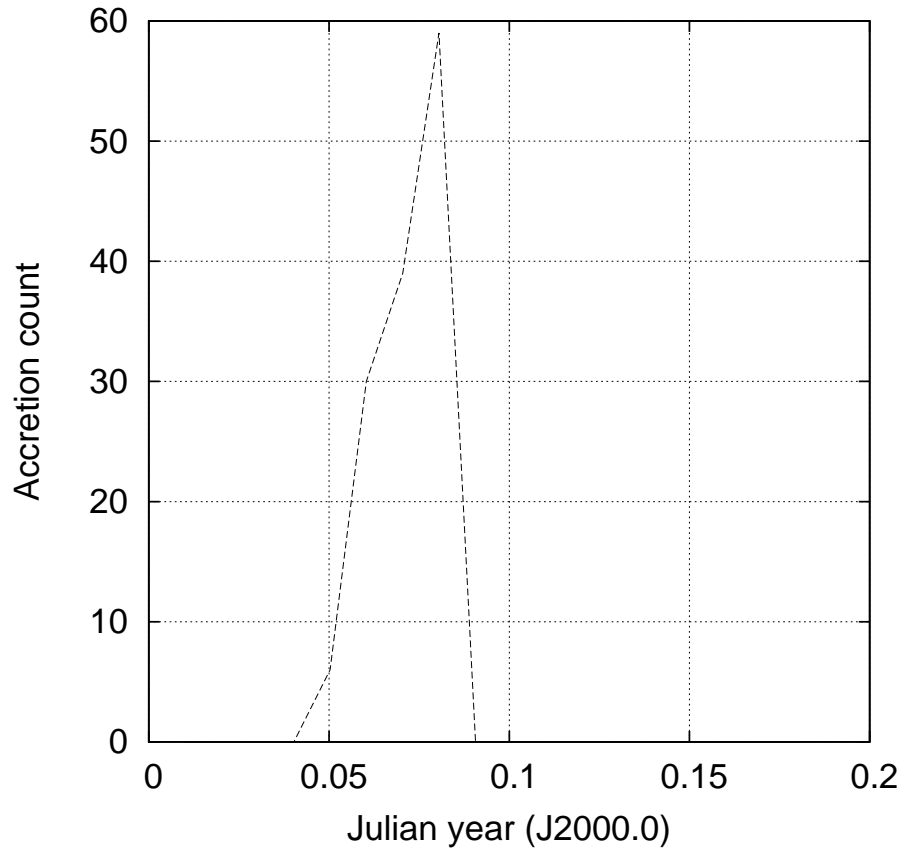


Fig. 6.— Accretion counts of the secondary (dashed line) in a simulation of a secondary colliding with a spherical particle cloud of radius 300 AU orbiting the primary.

In the first, we simulated a disk surrounding the secondary to establish the tidal effect of the primary on the accretion rate of the secondary. The disk was simulated with 10^4 particles positioned in a constant planar density disk in the xy -plane. The radius of the disk was set to 150 AU, comparable to the tidally stable radius of $\sim 50 r_{\text{sec}} \sim 140$ AU. This configuration was simulated for approximately two secondary periods. The resulting accretion rates are illustrated in Figure 5. The quiescent secondary accretion rate is greatly enhanced by the tidal action of the primary during the close pericenter passage. At this point, most of the disk is disturbed and accreted by the secondary in a time scale of approximately 0.5 yr.

In the second simulation, we used a spherical cloud of 10^4 massive particles, set at $z = 4000$ AU with a keplerian rotation around the primary, positioned so that it collides with the secondary. The radius and total mass of the sphere were set to 300 AU and $16 M_{\odot}$, respectively, matching the theoretical predictions in the next section. Figure 6 graphs the secondary accretion resulting from the collision. We find that the collision induces a brief peak in the secondary accretion rate, with a timescale of ~ 0.03 yr. This corresponds well with the theoretical prediction in the next section.

5. Discussion

The simplest explanation of the above results is that the secondary is impacting a thicker structure than the thin α -disk used in this simulation, and in much of the principal theoretical considerations and simulations concerning OJ 287, such as Ivanov et al. (1998).

A plausible additional structure is a geometrically thick but optically thin disk, such as the Polish doughnut model (Abramowicz et al. 1978; Kozłowski et al. 1978; Jaroszynski et al. 1980; Paczyński and Wiita 1980). In this model, the equipressure surfaces of the

accretion disk can be obtained by solving

$$\frac{d\theta}{dr} = -\frac{\partial_r g^{tt} - 2l\partial_r g^{t\phi} + l^2\partial_r g^{\phi\phi}}{\partial_\theta g^{tt} - 2l\partial_\theta g^{t\phi} + l^2\partial_\theta g^{\phi\phi}}, \quad (6)$$

where (t, r, θ, ϕ) are the usual Schwarzschild coordinates, $g^{\alpha\beta}$ are the components of the inverse of the metric and l is the specific angular momentum of a fluid element. Equation (6) can be solved analytically for a Schwarzschild metric if a constant angular momentum $l = l_0$ is assumed. The result is

$$\frac{1}{\sin^2(\theta)} = -\frac{r^2[1 + 2C_0(1 - r)]}{l^2(1 - r)}, \quad (7)$$

where r is in units of Schwarzschild radii and C_0 is the integration constant enumerating the equipressure surfaces. Figure 7 shows a model fit of this equation to the model coordinates of the precursor flares. Even though the fit describes a model with a nonrotating primary, the change in the equipressure surfaces for a rotating primary is not dramatic, as can be seen e.g. in Qian et al. (2009).

Thus a reasonable possibility is a model with a cool, geometrically thin accretion disk with a hot, geometrically thick corona. Additionally, the periodical impacts of the secondary tear off gas clouds from the accretion disk of the primary. Thus the corona of the primary's accretion disk is expected to be partly composed of gas clouds, as in the model of Svensson & Zdziarski (1994).

In this model of precursor bursts we are observing a brightening of the secondary black hole, not the primary. How can the secondary of mass $1.4 \times 10^8 M_\odot$ exceed the brightness of the primary of mass $1.84 \times 10^{10} M_\odot$? The key is the relative spin rate χ which is $\chi \sim 0.28$ for the primary and, quite reasonably, as will be shown, $\chi \sim 1$ for the secondary. The jet brightness of an accreting black hole with a jet is very sensitive to χ such that large χ systems are very much brighter than low χ systems of otherwise similar physical parameters. The jets of the two black holes would be aligned, as the jet direction

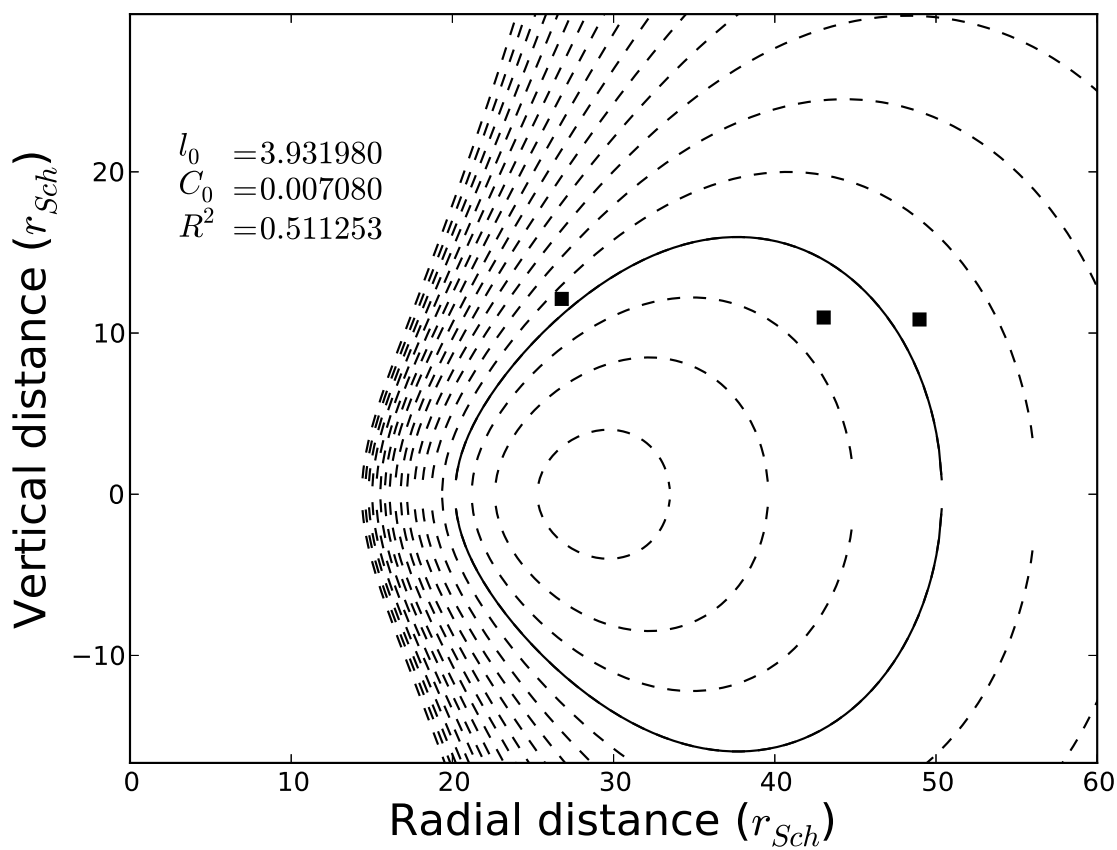


Fig. 7.— Best fit of equation (7) to model precursor coordinates (thick line). The best fit values of C_0 , and l_0 are indicated, as is the goodness of the fit R^2 . Additional equipressure surfaces with C_0 ranging from $[0, 2]$ times the best fit value (dashed lines) are also shown.

is strongly influenced by the magnetic field of the primary accretion disk (Palenzuela et al. 2010a,b). Thus both jets should have similar Doppler boosting factors.

We may additionally consider the secondary impact with a coronal gas cloud in more detail. From (Lehto & Valtonen 1996) we find the initial volume of the gas clouds torn from the accretion disk of the primary by the secondary during impacts to be

$$V_0 = \frac{\pi}{7} \eta^2 r_{\text{sec}}^2 h, \quad (8)$$

where r_{sec} is the Schwarzschild radius of the secondary black hole, h the primary accretion disk scale height and $\eta = (c/v_{\text{rel}})^2$ is a parameter of interaction, while c and v_{rel} are the speed of light and the velocity of the secondary relative to the disc, respectively. The disk thickness is a function of the accretion rate \dot{M} of the primary black hole (Stella and Rosner 1984). This rate is not well known since the observed emission of OJ 287 is jet-dominated, and the underlying disc-emission is not directly observed. Based on the strength of the emission lines (Sitko & Junkkarinen 1985) and the observed (beamed) luminosity of $\sim 2 \times 10^{46}$ erg/s in the radio-UV range the value of disc luminosity may be $\sim 2 \times 10^{45}$ erg/s (Worrall et al. 1982) which indicates $\dot{M} \sim 0.8 \times 10^{-3} \dot{M}_{\text{Edd}}$. \dot{M}_{Edd} is the accretion rate of the primary that would give the Eddington luminosity for it. In the following we will assume this accretion rate of the primary.

Further, c/v_{rel} lies approximately in the range of 4–12; for the impacts we are discussing here $c/v_{\text{rel}} \sim 6$. Thus we may take $\eta^2 \sim 1.3 \times 10^3$. With $r_{\text{sec}} = 4.2 \times 10^{13}$ cm we may calculate V_0 , and assuming that the initial cloud is spherical, its radius is $R_0 \sim 15$ AU. In the disk model of Sakimoto & Coroniti (1981) with the scaling from Stella & Rosner (1984), we get the surface mass density of $\Sigma_0 \sim 10^5$ g/cm². The exact value depends on the viscosity parameter α_g which is not known. Here we adopt $\alpha_g = 0.5$ which may not be unreasonable (King et al. 2007; Ogilvie & Dubus 2008; Carciofi et al. 2012). After the initial impact, the cloud will expand by a factor of k . When the secondary impacts this

cloud again, the mass of the column interacting with the secondary may be approximated as

$$\Delta m = \Sigma(\eta r_{\text{sec}})^2 = \Sigma_0 r_{\text{sec}}^2 \eta^2 k^{-2}, \quad (9)$$

where $\Sigma \propto k^{-2}$ is the surface mass density of the gas cloud after it has fully expanded and has reached the pressure balance with the hot corona. We obtain $\Delta m \sim 100k^{-2} M_{\odot}$. The secondary crosses the extent of the cloud in a timescale of $t_c \sim R_0 k / v_{\text{rel}} \sim 1.5 \times 10^{-3} k$ yr. Here the difficulty lies in obtaining an estimate for the expansion factor k of the cloud. Following Lehto & Valtonen (1996) we may estimate it to be at least $k = \tau^{4/7} \sim 14$, where τ is the initial average optical depth of the cloud, for at this point the cloud turns optically thin and an outburst is observed. Thereafter the optical light curve follows emission from an adiabatically expanding cloud; thus $k \sim 20$ at the time when the optical outburst is over. What happens thereafter is not known from observations, but it is possible that the cloud cools rapidly by radiation and may not expand very much again. We obtain the estimates

$$\Delta m \sim 0.25(k/20)^{-2} M_{\odot} \quad (10a)$$

$$t_c \sim 0.03(k/20) \text{ yr} \quad (10b)$$

$$\frac{\Delta m / t_c}{\dot{m}_{\text{Edd}}} \sim 8(k/20)^{-3}. \quad (10c)$$

Here $\dot{m}_{\text{Edd}} \sim 1 M_{\odot}/\text{yr}$ is the Eddington accretion rate of the secondary, assuming that the efficiency factor of the accretion process $\epsilon = 0.3$. This accretion rate gives the secondary the luminosity of L_{Edd} . The timescale estimate is in agreement with the simulation result obtained in the previous section for $k = 20$.

Most of the accreted matter will end up in a disk, and will be transferred to the secondary black hole only slowly, in time which exceeds the orbital period by orders of magnitude. We would expect the immediate outburst only from matter which falls straight into the innermost disk of the secondary, say, within $\sim 3r_{\text{sec}}$ of the secondary black hole. This matter flow is only about $1/\eta \sim 1/36$ of the flow calculated above, and thus we expect

outbursts of roughly $0.25(k/20)^{-3} L_{\text{Edd}}$ during the transit of the secondary through the gas cloud. The result scales with $\alpha_g^{-0.8}$; thus it could not be much smaller than our estimate but could possibly be bigger by a large factor, as α_g values down to ~ 0.1 have been reported (King et al. 2007). Thus, the secondary could possibly accrete close to the Eddington rate \dot{m}_{Edd} , which would in turn indicate luminosity not so far from the Eddington value of $L_{\text{Edd}} = 2 \times 10^{46}$ erg/s.

Here we have assumed that the matter falling at or near the inner edge of the accretion disk is transferred to the secondary black hole and its jet in a timescale $\lesssim t_c$. This would not be the case in the standard steady accretion process where the timescale is of the order of ~ 1000 yr. However, it has been demonstrated that the accretion timescale is much faster than the standard steady rate when we are considering accretion of magnetic flux to the jet where the relevant timescale for matter falling near r_{ISCO} is of order ~ 10 orbital periods, or even less (Krolik et al. 2005). For the secondary this is equivalent to a timescale of ~ 7 days. However, magnetohydrodynamic accretion is under intense study, and it is difficult to be very specific about the time scale at this time (Beckwith et al. 2009). Fast timescales have also been demonstrated in the case when a strong tidal perturbation applies to the disk (Byrd et al. 1986, 1987; Lin et al. 1988; Goodman, J. 1993). In this case it is the tidal perturbation of the primary on the secondary disk which causes accretion in the orbital timescale of the inner disk, i.e. in a timescale of a few days.

The last element of the model that needs to be considered in detail is the spin of the secondary component. We propose that the binary model naturally leads to a high present time spin value of the secondary. First, we note that the Sakimoto–Coroniti disk model is gravitationally unstable at distances over ~ 2 pc for the OJ 287 primary (Sakimoto & Coroniti 1981). However, during the coalescence of a supermassive black hole binary with a large mass ratio, the binary is expected to spend a longer time at smaller separations,

or that the evolution would stall in what is known as the "final parsec problem" (Berczik et al. 2006). A recent study by Iwasawa et al. (2011) uses a theoretical prediction by Matsubayashi et al. (2007) to calculate that a coalescing supermassive black hole binary of a comparable mass ratio to OJ 287 would reach a semi-major axis of 2 pc in $\sim 5 \times 10^7$ yr starting from an initial semi-major axis of 20 pc. Based on numerical work they find the total merger timescale to be greater than $\sim 2.5 \times 10^8$ yr, for a system with parameters like OJ 287, which thus leaves at least 2.0×10^8 yr for the secondary to accumulate spin through accretion of matter from the accretion disk of the primary.

The accretion spin-up timescale can be estimated from the results initially derived in Bardeen (1970) and further elaborated in Thorne (1974). As the estimate of the current mass of the secondary is $1.4 \times 10^8 M_\odot$, the amount of rest mass it must have accreted to reach a spin of $\chi \sim 1$ is $\sim 1 \times 10^8 M_\odot$. By the reasoning above and in Lehto & Valtonen (1996), we would expect a mass of $2\Sigma\eta r_{\text{sec}}^2$ to be accreted by the secondary during one period P , which leads to a fiducial accretion rate of $\dot{M} = 2\Sigma\eta r_{\text{sec}}^2/P$. The scaling in Stella & Rosner (1984) gives $\Sigma \propto r^{-3/5}$ at larger distances, and for the rest $\eta \propto P^2 \propto r^3$. Using the values at $\Sigma_0 = 10^5$ g/cm², $\eta_0 = 36$ and $P_0 = 12$ yr at $r = r_0 = 10^4$ AU, we find $\dot{M} \sim 0.5(r/r_0)^{9/10} M_\odot/\text{yr}$. Thus we would expect the accretion rate to have been larger in the past, though considering the growth of eccentricity documented in Iwasawa et al. (2011), the impacts of the secondary have been at a distance of $\sim r_0$ during most of the orbital evolution. Thus using the value $\dot{M} = 0.5 M_\odot/\text{yr}$ leads to an upper limit estimate of the spin-up timescale of $10^8 M_\odot/\dot{M} \sim 2 \times 10^8$ yr, which is in line with the estimated time available for the accretion to occur. Further, it is possible that the orbital plane of the secondary may have been closer the plane of the accretion disk of the primary before, having attained the current value of inclination at $\sim 90^\circ$ at a later time, as evidenced by the evolution of inclination in Iwasawa et al. (2011). This would have increased the accretion by the secondary, and further shortened the spin-up timescale. Based on these

considerations we would expect the secondary in the binary black hole model to have a high spin, at least compared to the primary spin value.

The resulting luminosity for the secondary is then comparable to the maximum bremsstrahlung luminosity arising from the hot bubbles torn off the disk (Ivanov et al. 1998) or the luminosity of the primary accreting at the rate of $\sim 10^{-3}\dot{M}_{\text{Edd}}$, amplified by a reasonable forward beaming Doppler factor. Since the primary and secondary are expected to have similar Doppler boosting factors, precursor flares originating from the secondary black hole could reasonably exceed the primary black hole luminosity for brief periods. As such, the case for precursor flares originating from the secondary is quite plausible.

One of the best ways to verify the presence of the secondary jet in the radiation of OJ 287 is to look for the shortest variability timescale. It should be related to the orbital period of the innermost stable circular orbit in the co-rotating case which is approximately 3.8 hours for the secondary, and 100 days for the primary. Due to Doppler boosting in the jet, variability time scales down to about 15 minutes may appear in the secondary jet and about 5 days in the primary jet. Therefore during secondary bursts the variability may be especially rapid. Some evidence for this has been seen in the light curve of OJ 287 prior to the 1983 great outburst (Valtaoja et al. 1984).

Considering that the semi-major axis of the system corresponds to an observed angular diameter of ~ 0.01 mas, it might be possible to follow the orbital motion of the binary in the sky. This requires observational capabilities to progress to a spatial resolution at 10 microarcsecond level, possible with e.g. the GRAVITY instrument (Eisenhauer et al. 2011). In addition to directly confirming the binary nature of the system, this would allow explicit coordination of light curve events with the phase of the binary orbit.

6. Conclusions

We have studied three precursor flares in the light curve of OJ 287. We propose a model where these outbursts are caused by the secondary black hole impacting on a thick disk of the primary before the actual impact on the primary accretion disk. The precursor outburst is triggered by gas falling into the secondary black hole leading to its jet brightening.

Using this model we predict a new precursor flare of to occur around 2020.96, with a brightness of approximately 2 mag above the quiescent level. It would be especially interesting to look for intra-day variability during this outburst. Also we expect that intra-day variability will appear prominently in smaller outburst events between now and September 2013 when the secondary hits the primary accretion disk, and moves to the far side of the disk as seen by us.

P. Pihajoki acknowledges the support of Turku University Foundation (grant no. 7642) and Magnus Ehrnrooth foundation (grant no. Ta2012n6).

This work has been partly supported by the Polish MNiSW grant under the contract No. 3812/B/H03/2009/36.

Table 1. Observations of the 2012 precursor flare.

MJD	Location	Band	Mag.	Mag. error
55112.2675400	KVA	R	14.107	0.027
55113.2541600	KVA	R	13.921	0.019
55118.2574200	KVA	R	14.089	0.018
55120.2617300	KVA	R	13.993	0.018
55126.2527500	KVA	R	13.468	0.018

Note. — Table 1. is published in its entirety in the electronic edition of The Astrophysical Journal. A portion is shown here for guidance regarding its form and content.

REFERENCES

- Abramowicz, M., Jaroszynski, M. & Sikora, M. 1978, *A&A*, 63, 221
- Anupama, G.C., Kembhavi, A.K., Prabhu, T.P., Singh, K.P. & Bhat, P.N. 1994, *Astron. Astrophys. Suppl. Ser.*, 103, 315
- Baliyan, K.S., Joshi U.C. & Ganesh S. 2005, *BASI*, 33, 181
- Bardeen, J.M. 1970, *Nature*, 226, 64
- Beckwith, K., Hawley, J.F. & Krolik, J.H. 2009, *ApJ*, 707, 428
- Berczik, P., Merritt, D., Spurzem, R. & Bischof, H. 2006, *ApJ*, 642, L21
- Budyn, M., Zola, S. & Wojcik, K. 2010, *ASPC*, 435, 87
- Byrd, G.G., Valtonen, M.J., Valtaoja, L. & Sundelius, B. 1986, *A&A*, 166, 75
- Byrd, G.G., Sundelius, B. & Valtonen, M. 1987, *A&A*, 171, 16
- Carciofi, A.C. et al. 2012, *ApJ*, 744, L15
- Chandra, S., Baliyan, K.S., Ganesh, S. & Joshi, U.C. 2011, *ApJ*, 731, 118
- Eisenhauer, F. et al. 2011, *The Messenger*, 143, 16
- Fiorucci, M. & Tosti, G. 1996, *Astron. Astrophys. Suppl. Ser.*, 116, 403
- Gezari, S. et al. 2012, *Nature*, 485, 217
- Gonzalez-Perez J.N., Kidger M.R. & Martin-Luis F. 2001, *AJ*, 122, 2055
- Goodman, J. 1993, *ApJ*, 406, 596
- Hawley, J.F. & Krolik, J.H. 2006, *ApJ*, 641, 103

- Ivanov, P.B., Igmenshev, I.V. & Novikov, I.D. 1998, *ApJ*, 507, 131
- Iwasawa, M. et al. 2011, *ApJ*, 731, L9
- Jaroszynski, M., Abramowicz, M.A. & Paczyński, B. 1980, *Acta Astron.*, 30, 1
- Jester, S. et al. 2005, *AJ*, 130, 873
- Kidger, M.R., & Takalo, L.O. 1993, *IAU Circ.*, 5909, 1
- Kidger, M.R. et al. 1994, *Intensive Monitoring of OJ287*, eds. M.R. Kidger & L.O. Takalo, Tuorla Observatory Rep. 174, 106
- Kidger, M.R. et al. 1995, *Astron. Astrophys. Suppl. Ser.*, 113, 431
- King, A.R., Pringle, J.E. & Livio, M. 2007, *MNRAS*, 376, 1740
- Kozłowski, M., Jaroszynski, M. & Abramowicz, M.A. 1978, *A&A*, 63, 209
- Krolik, J.H., Hawley, J.F. & Hirose, S. 2005, *ApJ*, 622, 1008
- Landolt A.U. 2009, *AJ*, 137, 4186
- Lehto, H.J., & Valtonen, M.J. 1996, *ApJ*, 460, 207
- Lin, D.N.C., Pringle, J.E. & Rees, M.J. 1988, *ApJ*, 328, 103
- Matsubayashi, T., Makino, J. & Ebisuzaki, T. 2007, *ApJ*, 656, 879
- Miller, R.H. 1976, *J.Comput.Phys.*, 21, 400
- Neilsen, D. et al. 2011, *Proc. Nat. Acad. Sci.*, 108, 12641
- Ogilvie, G.I. & Dubus, G. 2008, *MNRAS*, 320, 485
- Paczyński, B. & Wiita, P.J. 1980, *A&A*, 88, 23

- Palenzuela, C., Garrett, T., Lehner, L. & Liebling, S.L. 2010a, *Phys.Rev.D*, 82, 44045
- Palenzuela, C., Lehner, L. & Liebling, S.L. 2010b, *Science*, 329, 927
- Qian, L. et al. 2009, *A&A*, 498, 471
- Sagar, R., Stalin, C.S., Gopal-Krishna & Wiita, P.J. 2004, *MNRAS*, 348, 176
- Sakimoto, P.J., & Coroniti, F.V. 1981, *ApJ*, 247, 19
- Shakura, N.I., & Sunyaev, R.A. 1973, *A&A*, 24, 337
- Sillanpää, A., Haarala, S., Valtonen, M.J., Sundelius, B. & Byrd, G.G. 1988, *ApJ*, 325, 628
- Sillanpää et al. 1996a, *A&A*, 305, L17
- Sillanpää et al. 1996b, *A&A*, 315, L13
- Sitko, M.L. & Junkkarinen, V.T. 1985, *PASP*, 97, 1158
- Stella, L., & Rosner, R. 1984, *ApJ*, 277, 312
- Thorne, K.S., 1974, *ApJ*, 191, 507
- Sundelius, B., Wahde, M., Lehto, H.J. & Valtonen, M.J. 1996, *Blazar Continuum Variability*,
ASP Conf. Ser., 110, 99
- Sundelius, B., Wahde, M., Lehto, H.J. & Valtonen, M.J. 1997, *ApJ*, 484, 180
- Svensson, R., & Zdziarski, A.A. 1994, *ApJ*, 436, 599
- Valtaoja, E. et al. 1984, *Nature*, 314, 148
- Valtonen, M.J. & Lehto, H.J. 1997, *ApJ*, 481, L5
- Valtonen, M.J. et al. 2006a, *ApJ*, 643, L9

Valtonen, M.J. et al. 2006b, ApJ, 646, 36

Valtonen, M.J. 2007, ApJ, 659, 1074

Valtonen, M.J., Kidger, M., Lehto, H. & Poyner, G. 2008a, A&A, 477, 407

Valtonen, M.J. et al. 2008b, Nature, 452, 851

Valtonen, M.J. et al. 2009, ApJ, 698, 781

Valtonen, M.J. et al. 2010a, ApJ, 709, 725

Valtonen, M.J. et al. 2010b, Cel. Mech. Dyn. Astr., 106, 235

Valtonen, M.J. et al. 2011, ApJ, 742, 22

Worrall, D.M. et al. 1982, ApJ, 261, 403